Engineering Geology 286 (2021) 106073

Contents lists available at ScienceDirect

Engineering Geology

journal homepage: www.elsevier.com/locate/enggeo

Multi-proxy analysis of boreholes in remolded Quaternary paraglacial deposits (Avignonet landslide, French Western Alps)

Grégory Bièvre *, Christian Crouzet

Univ. Grenoble Alpes, Univ. Savoie Mont Blanc, CNRS, IRD, Univ. Gustave Eiffel, ISTerre, 38000 Grenoble, France

ARTICLE INFO

Keywords:
Landslide
Paraglacial Quaternary sediments
French western Alps
Sedimentary compaction
Boreholes

ABSTRACT

The Avignonet landslide in the Trièves area is made of Quaternary paraglacial sediments among which imbricated till, glacio-lacutrine and fluviatil layers. Numerous boreholes (drillings and corings) were conducted during the mid-1980s and the mid-2000s to assess the geological and geotechnical setting of the inhabited, southern part of this slow-moving earthslide. Heterogeneous paramaters available from these different boreholes make interpretation difficult. Gamma-ray logging along with magnetic susceptibility and pocket vane tests on core samples allowed to distinguish between the different lithological and geotechnical units. Mechanical strength obtained from drilling parameter recording acquired during drilling was correlated to corings and their combination, along with outcrop observations, was used to delineate the lithological units and shear surfaces.

The joint analysis of the dataset with outcrop observations and chronological data reveals a high geological complexity with the intrication of various sedimentary units. Two ancient landslides, several tens of metres in width, were furthermore identified within the large Avignonet landslide, almost 2 km in width. All the results point toward a high lithological and hydrogeological complexity that impacts the dynamics of the landslide. This work shows the interest of a multi-proxy approach in studies involving Quaternary sedimentary units. The methodology developed here could be applied to other sites with different palaeoenvironmental contexts initially exhibiting sedimentary compaction, such as lacustrine or coastal environments.

1. Introduction

The Trièves and Beaumont areas (TL and BL in Fig. 1, respectively) in the French western Alps are characterized by the presence of Quaternary glacio-lacustrine clays that have been since long submitted to important landslides. These Quaternary deposits have been studied from a geological point of view since the XIXth century, and an important literature, mainly in French, is devoted to their sedimentological and palaeoenvironmental setting (Lory, 1858; Monjuvent, 1973; Huff, 1974). The first historical occurrence of a landslide in the area seems to be reported in a local newspaper around 1850 when the village of Avignonet, North of the Trièves area, was washed out by a landslide to the bottom of the valley (unsourced local newspaper in Blanchet, 1988). Large circular scarps up to about 1.8 km in diameter delimit these landslides. They can be observed on ancient aerial photographs from the 1940s and also on Ordnance Survey maps from the 1850s (IGN, 2019). Large landslides are currently active all over the area and pose numerous problems in terms of land use and safety. As such, numerous geotechnical investigations were carried out and several publications depict and characterize the geotechnical properties of the glacio-lacustrine deposits in the Trièves and Beaumont areas (among others, Caris and Van Asch, 1991; Van Asch et al., 1996). In the past fifteen years, significant efforts were made to develop the use of geophysical imaging methods to characterize the geometry and the internal structure of these clayey landslides. Using shear wave velocity, it was possible to image the palaeoenvironmental setting of the Avignonet and Harmalière landslides (Bièvre et al., 2011) and to image the 3D geometry of the Avignonet landslide (Renalier et al., 2010b). Electrical resistivity allowed to detect lithological interfaces within the Avignonet landslide (Bièvre et al., 2016). These geophysical methods, however, need to be calibrated with direct data. These lasts can originate from field observation (outcrops) and/or from boreholes. Boreholes are classically operated during geotechnical studies (drilling, coring, auger, etc.) to provide the parameters required for stability analysis and geotechnical design (number and depth of shear surfaces and lithological units, location of the water table, unit weight of the soil, cohesion and friction angle, etc.). Boreholes allow to identify lithology and to establish lateral correlations (Lee et al., 2012), to get samples for identification and mechanical tests

* Corresponding author.
E-mail address: gregory.bievre@univ-grenoble-alpes.fr (G. Bièvre).

https://doi.org/10.1016/j.enggeo.2021.106073
Received 14 September 2020; Received in revised form 23 February 2021; Accepted 26 February 2021
Available online 5 March 2021

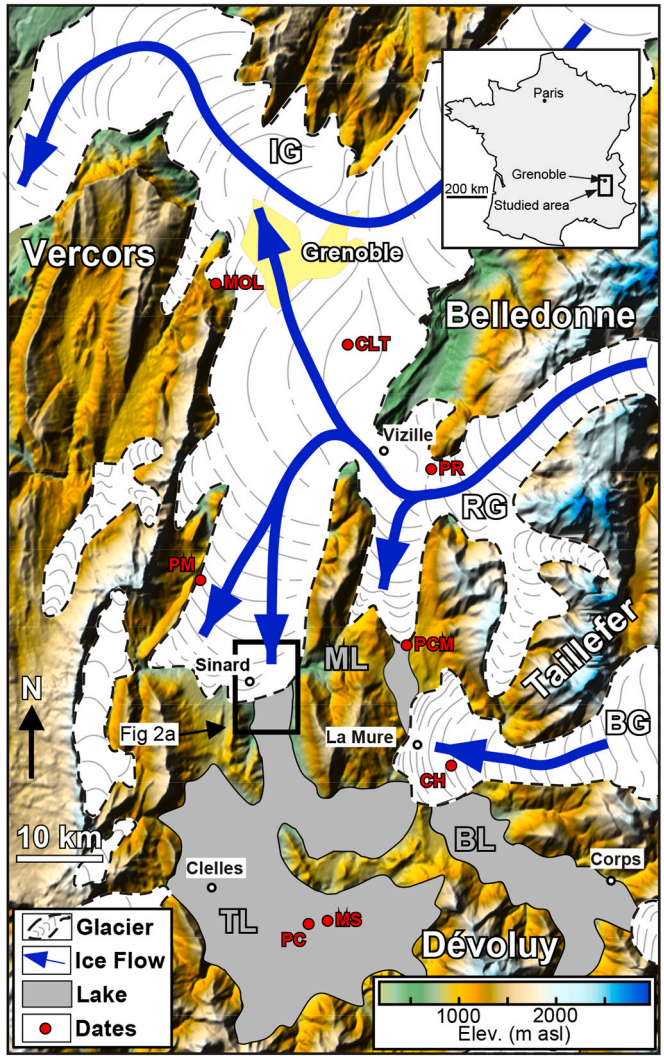

Fig. 1. Location of the study site and regional palaeogeographic situation during the Last Glacial maximum, adapted from Monjuvent (1973) with ice flow from Coutterand (2010). IG: Isère glacier; RG: Romanche glacier; BG: Beaumont glacier; TL: Trièves lake; ML: Matheysine lake; BL: Beaumont lake; ML: Mousterian lithics; CLT: Crey alluvial terrace; PR: polished rock; PM: Prélenfrey moraine; PCM: Pierre-Châtel moraine; CH: Charlaix laminated clays; MS: mollusc shells; PC: Pompe Chaude.

(Renalier et al., 2010a) and, finally, to detect and monitor the dynamics of shear surfaces (with inclinometers) and water table (with piezometers) at depth (Uhlemann et al., 2016). Complimentary logging operations can be conducted to valorize boreholes (Bièvre et al., 2012; Lofi et al., 2012). On the one hand, boreholes provide direct and high resolution data. On the other hand and contrary to geophysical measurements that can provide spatially continuous images, boreholes remain punctual in space. Furthermore, it is worth trying to get the maximum possible data from these expensive reconnaissance operations. Curzi et al. (2017) used 2 corings to establish a sedimentological model in the Adriatic sea coastal environment in Italy. Facies analysis along with datings allowed to reconstruct the palaeoenvironmental succession. Adjacent piezocone tests were further used to establish correlations with corings and, then, piezocone tests conducted over the study site were finally used to build an integrated sedimentological and geotechnical characterization of the site with a better understanding of local site conditions for land use and planning.

Among the description of lithological units, quantitative data from core analysis generally encompass identification parameters such as water content, unit weight, grain size, etc. (Meisina, 2006). More complete quantitative data are very partially covered in the literature devoted to landslides. Picarelli et al. (2005) showed that mechanical tests conducted with pocket devices along core samples from Italian mudslides allow the detection of shear surfaces, which present weak undrained shear strengths along with high water content. Other reconnaissance tools include in situ tests such as penetration tests (cone penetration test, piezocone, seismic cone penetration test, etc.; Hunt, 2007; Cai et al., 2010). However, empirical relationships are required to relate the measured parameters to a geotechnical parameter of interest such as the undrained cohesion. Vane shear tests are less employed but provide directly mechanical parameters for geotechnical studies. Finally, pressuremeter tests are also commonly used by the geotechnical engineering community for prospecting and design but are poorly reported in the geological literature.

Among the difficulty to relate the abovementioned parameters to the lithology in individual boreholes, it is also highly complex to establish lateral correlations between boreholes in Quaternary formations deposited in glacial environments. This difficulty arises from the 3D organisation of such deposits with facies variations occurring over short distances. Climatic variations also induce changes in palaeoenvironments and in the nature of sediments implying vertical lithological and therefore geotechnical heterogeneities in borehole (Curzi et al., 2017). Finally, the occurrence of landslides on such sites introduces another degree of complexity, with the mobilization and displacement of large volumes of material alongslope.

The present study focuses on the Avignonet/Sinard area in the Trièves area (French western Alps) and the use of multi-proxy investigations in order to reconstruct the geometry of the lithological units and to evidence present-day and ancient landslide activity. This is achieved mainly by the recognition of lithological units and shear surfaces in 10 boreholes. Since geotechnical investigations were carried out by different teams and companies since the end of the XXth century, the available data are highly heterogeneous and building a homogeneous dataset remains challenging. Complimentary to boreholes conducted for geotechnical studies, several boreholes were conducted to calibrate geophysical data and each one underwent various tests. The objective of this paper is to expose new geological and geotechnical observations provided by borehole campaigns which were not exploited beyond the classical engineering approach and to show how these new observations, obtained by relatively classical techniques, are able to complement the established geotechnical and geological model of this area. This paper also aims at presenting proxies which have not been reported so far for landslide studies. Finally, dating was conducted when possible. Chronostratigraphic results are presented in the paper with the aim to show how they may help identifying ancient landslide activity and to establish lateral lithological and stratigraphic correlations.

2. Geological and geotechnical setting

The Trièves area is located approximately 50 km south of Grenoble in the SE part of France (Fig. 1). Most of the bedrock of the Trièves depression is made up of Callovo-oxfordian black shales. It is situated between the crystalline Taillefer massif to the East and the subalpine Vercors massif made up of Mesozoic marls and limestones to the West and, finally, by the Dévoluy massif made up of Senonian limestones to the South (Barféty and Debelmas, 1967; Pécher et al., 1988). It is a high-lying intra-mountain basin in which the Jurassic layers were covered by Quaternary loose sediments. Pre-Quaternary deposits form a vast monoclinal structure westward dipping in relationship with the uplift of the crystalline dome of La Mure to the East (western part of the Taillefer massif).

The Quaternary deposits have been extensively studied by Monjuvent (1973). As no important discovery has been made since, we refer to this seminal monograph. The Quaternary layers lie unconformably above the Jurassic bedrock. Several incisions in the bedrock were filled

up by massive gravel and pebble fluvial units, and were topped by marsh deposits evidenced by the occurrence of lignite. Those fluvial deposits are covered by glacigenic till, assumed to be contemporaneous with the global Marine Isotope Stadium 4 (MIS4). The Trièves area is characterized by the occurrence of large volumes of silt-clay sediments, up to more than 250 m thick locally: the glacio-lacustrine laminated clay (Huff, 1974). They evolve vertically and laterally to coarser deltaic deposits (sand and gravel). Deposits of more recent associated alluvial cones are observed in few places. Those clays are outcropping up to 750 m above sea level (asl). During the deposition of these sediments, the outlet of the catchment was dammed by the Romanche glacier coming from the North (Fig. 1). In the northern part of the Trièves area only, the lacustrine clay is covered by till (Fig. 2a) brought by the glacier coming from the north (Fig. 2b). The study site is located in the southern part of the Avignonet landslide (Fig. 2c). Geotechnical prospecting was concentrated in this area because it is inhabited.

The precise chronology of the glacio-lacustrine deposits is not well known. No plant remains were ever found in place in the sedimentary units. Therefore, indirect observations are required. As the dam is thought to be the glacier itself, time of deposition is associated to the Last Glacial Maximum (LGM). In the studied area, the age of the maximal extension of the glacier is still debated: should it correspond to the global LGM or may it be older? Twenty dates were found in the literature, which were mainly published in French between the late 1960s and 1980s. They were carefully checked and ^{14}C ages were re-processed using the methodology exposed further in the Materials and

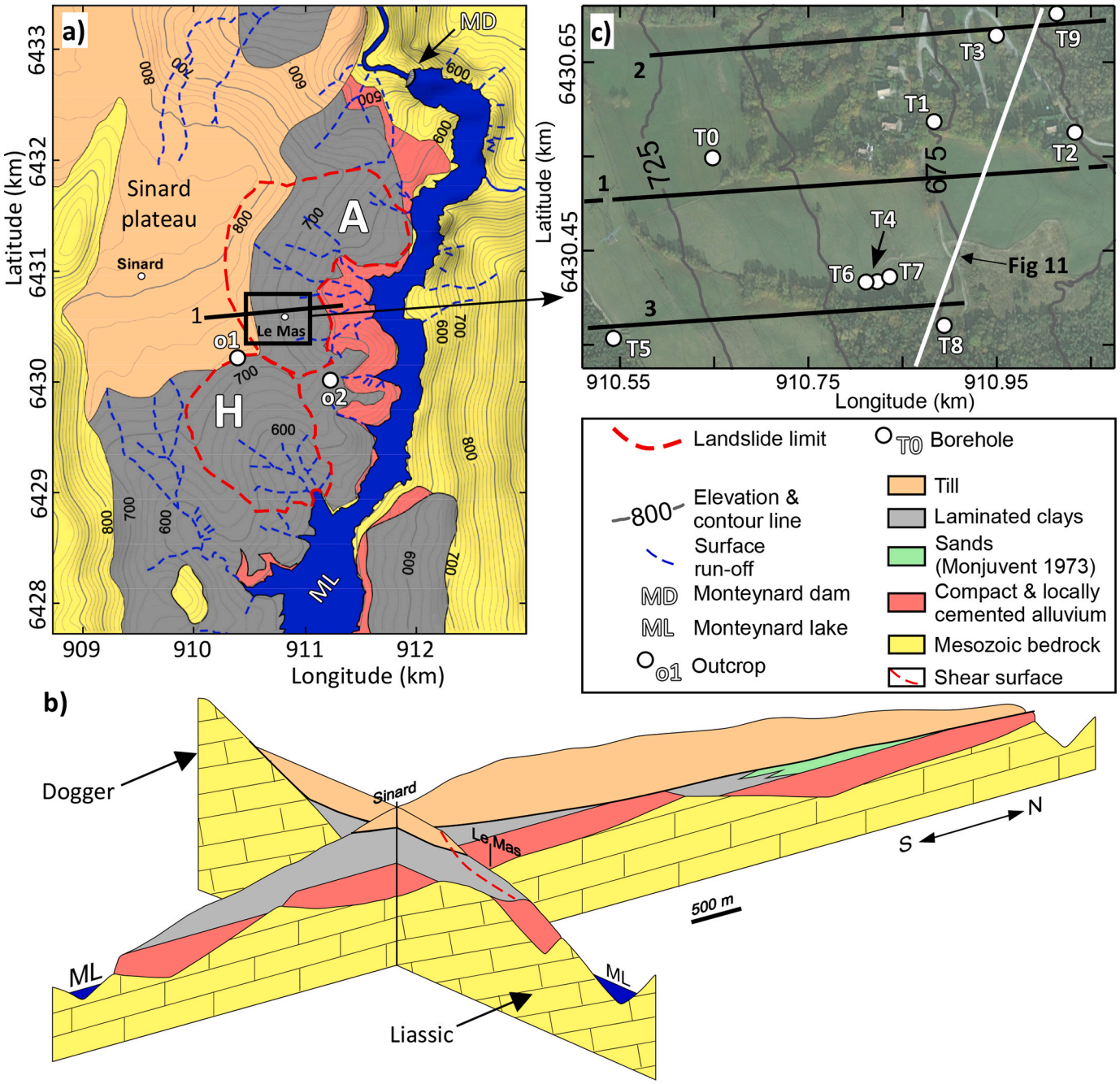

Fig. 2. Presentation of the study area. a) Geological map and location of the Avignonet (A) and Harmalière (H) landslides. Black line 1: geological cross-section in Fig. 10b. Map modified from Bièvre et al. (2016). b) Fence diagram showing the geometrical arrangement of the quaternary units. Geological cross-sections adapted from Monjuvent (1973). c) Close-up on the southern part of the Avignonet landslide with the location of boreholes T0 to T9. 1, 2 and 3: cross-sections in Fig. 10.

methods section. In order not to extend the present paper, a synthesis is provided hereafter and all the details and bibliographic references are provided in Supplementary Information S-1.

In the southern part of the Trièves area, several attempts were performed to constrain the age of fluvial deposits underlying the lacustrine clays. U/Th on mollusc shells (MS in Fig. 1) indicate ages around 70 ka. ^{14}C dates on wood and lignite fragments at the same site are all within or beyond the limit of the method. This is confirmed by a new test we performed (see sample Poz-96,636 in Supplementary Information S-1). A sandy lens outcropping in the Pierre Châtel moraine (PCM in Fig. 1), which is the most external one, was dated using Optically Simulated Luminescence (OSL) method. It provided an age between 47 and 55 ka for the maximum glacial extension in the neighbouring Matheysine area. Other chronological constraints are scarce. South of Grenoble, at ca. 1050 m asl, Mousterian lithics (MOL in Fig. 1) were collected above a moraine, suggesting an age older than 40 ka for the glacial deposits. The discovery of wood fragments (crushed branches) dated older than 35 ka in a till in the Prélenfrey area (PM in Fig. 1) suggest the occurrence of a glacier during the MIS4. In the area of Grenoble, several wood fragments were collected in the Crey deltaic lacustrine terrace (CLT in Fig. 1) lying stratigraphically above a till. They provided ages between 24.7 and 34.3 ka cal BP for this kame terrace contemporaneous of a retrait stadial position of the glacier. On the other hand, cosmogenic dates suggest younger ages for the glacial retreat. A polished rock at 1120 m asl in the northern Romanche valley was exposed since 17.5 ± 1.1 ka (PR in Fig. 1). ^{10}Be concentration vs. depth profiles in several palaeoterraces of

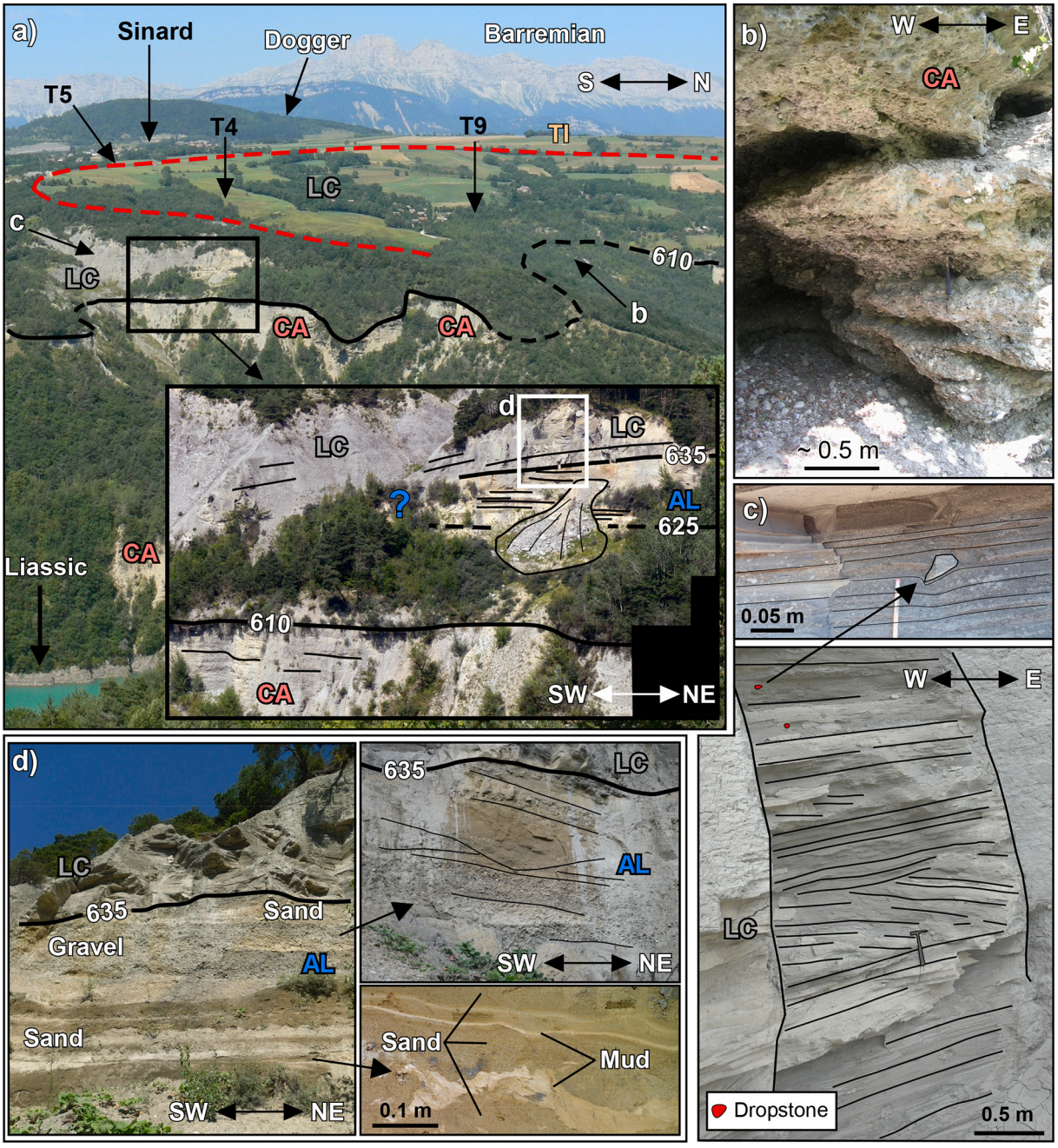

Fig. 3. Panoramic view of the study site and detailed views of outcrops. a) Panoramic view of the site. CA: cemented fluvial alluvium; LC: laminated clays; AL: uncemented fluvial alluvium; TI: till. A close-up on outcrop o2 is embedded. b) Detailed view of the locally cemented alluvium (palaeoterrace A2 here). c) Laminated clays with dropstones. Note the presence of planar cross-bedding. d) Detailed view of the uncemented fluvial alluvium with sand and also mud clasts and mud lenses (indicative of synsedimentary deformation) at the base and sand and gravel at the top with erosive features.

the Drac river provide Holocene ages. Only the uppermost one, contemporary with the highest palaeolake level, exhibits age between 18.6 and 23 ka. As it is not the scope of the present paper, the discrepancy between, on the one hand, ^{14}C, ESR and U/Th dates and, on the other hand, OSL dates, will not be discussed. Ages obtained using the three first abovementioned techniques are in good agreement and they will be further considered as more probable than OSL ages.

Fig. 3a presents a panoramic view of the Avignonet landslide with the cemented fluvial alluvium (CA; detailed view in Fig. 3b) relying on the Jurassic bedrock, the laminated clays (LC; with dropstones and locally planar cross-bedding; Fig. 3c) and the till (TI). The subplot within Fig. 3a zooms on a new outcrop (o2) presenting alluvial and lacustrine deposits located stratigraphically ~15 m above the cemented alluvium. The base of the outcrop is made of lacustrine sand with dropstones, mud clasts and mud lenses indicative of synsedimentary deformation. Above are found alluvial layers of gravels and pebbles. The top of the unit is sandy and shows erosive features (channelling in the upper right part of Fig. 3c). Above an elevation of around 635 m asl, this unit passes without transition to lacustrine laminated clays. The lateral transition between this unit and the laminated clays cannot be observed in the field because of poor outcropping conditions (Fig. 3a). The laminated clay unit is then found up to an elevation of around 750 m asl, the last 50 m probably corresponding to lacustrine sediments enriched in coarser elements originating from a proximal position of the glacier (Bièvre et al., 2016). The top of the sedimentary sequence is made of a maximum of 50 m of till (Figs. 1c and 3a) and corresponds to the last advance of the glacier in the area. Such glacial deposits were better observed in coring and will be illustrated further.

From a geotechnical point of view, landslides in the Trièves (and Beaumont) area correspond to slow-moving landslides with sliding velocities ranging between a few mm/yr to several tens of cm/yr. Velocity is higher between November and April, highlighting a precipitation-driven control (Van Asch et al., 1996; Bièvre et al., 2018). These landslides generally correspond to earthslides with retrogression mechanisms at the headscarp (Hungr et al., 2014; Fiolleau et al., 2021). Some of them can evolve suddenly into earthflows, as it happened to the neighbouring Harmalière landslide (H in Fig. 1) in March 1981 and late June 2016, with measured displacements up to 50 m in 1 month (Lacroix et al., 2018). From a granulometric point of view, the so-called laminated clays are clayey silts and exhibit a porosity of ~40–45%. The phreatic water table is generally shallow (a few m deep, depending on the season) and the natural gravimetric water content w (30–35%) is close to the average Atterberg Liquid Limit (Wl) of 39% (Carrière et al., 2018). The laminated clays also have a narrow plasticity index (Ip) of 15–17%, which explains the propensity of these landslides to accelerate and possibly turn into earthflows, generally during rainy and snowy seasons. The landslides present several shear surfaces located at depths of generally 5 m, 10–15 m and 40–50 m (Jongmans et al., 2009).

3. Materials and methods

Most of the tests carried on the samples and in the boreholes are classical and their principles are described in numerous books (Clayton et al., 1995; Becker, 2001; Hunt, 2007). Only techniques less common to the engineering community will be described further.

3.1. Outcrop sampling

The main objective of outcrop sampling was to provide dates from the base to the top of the lacustrine sequence (elevations between around 635 m asl and 750 m asl). Alluvial layers at the base of the lacustrine sequence (~610–635 m asl) were sampled to perform Optically Simulated Luminescence (OSL) dating. Considering the maximum assumed age of the lacustrine deposits from literature (~50 ka), clayey samples were used to perform bulk radiocarbon dating. ^{14}C dating was also performed on core samples from laminated layers. Datings were conducted at ARTEMIS LMC-14 in France, except for 2 samples, namely plant remains in T4 and *Equisitum* Sp. at outcrop, processed in Poznan (Poland) and in Lyon (France), respectively. Radiocarbon ages were calibrated with the CALIB software (Stuiver and Reimer, 1993) using the Intcal13 calibration curve (Reimer et al., 2013). The reservoir effect induced by the lacustrine environment could not, however, be taken into account. A compilation of dates available at the regional scale is synthesized in Supplementary Table S1.

3.2. Measurements in boreholes and on samples: Drilling Parameter Recording (DPR), logging and laboratory tests

Geological and geotechnical observations conducted on 10 boreholes (T0 to T9) were used in this study and the different tests are exposed in Table 1 and located in Fig. 2. Following the reactivation of the neighbouring Harmalière landslide in March 1981, geotechnical studies started in 1982 to evaluate stability conditions in the hamlet of Avignonet where a housing program was in progress. Rotary drillings were operated by varying geotechnical companies and data synthesis and robustness requires a thorough revisit and evaluation, notably concerning geological descriptions and interpretations. Furthermore, measured parameters depend on the objective of each borehole and, as such, the available dataset is highly heterogeneous. Reconnaissance works started with drillings T0 and T3, and corings T1 and T2 (location in Fig. 2a), all of which were equipped with inclinometers (Table 1). T1 core samples were retrieved several decades after the drilling and, consequently, only limited measurements could be conducted on samples. T9 was conducted in 1986 to install a piezometer. Drilling Parameter Recording (DPR), namely the advance rate Ar (m/h), the drilling fluid pressure Df (bar) and the thrust pressure Tp (bar) were recorded for T0, T3 and T9. Since only scanned graphics were available, data were digitized with the WebPlotDigitizer online software (Rohatgi, 2019). The Somerton index Sd (expressed in bar or Pa; Somerton, 1959), indicative of the mechanical strength, was determined using the simplified relationship proposed by Laudanski et al. (2013):

$$Sd \approx \frac{Tp}{\sqrt{Ar}} \quad (1)$$

The Somerton index was analysed jointly with the drilling fluid pressure, indirectly related to the permeability of the sub-surface, to provide a geological/geotechnical interpretation. T4 was cored in 2007 and reached a depth of 49.3 m (and was further drilled down to 63 m). Classical identification tests were carried out (water content, unit weight, grain size, etc.). Undrained shear and compressive strengths (USS and UCS, respectively) were measured each 0.1 m with a pocket vane tester and a pocket penetrometer, respectively. In saturated conditions, the unconfined and undrained shear strength corresponds to the undrained cohesion Cu (Lade, 2001). Assuming undrained conditions for these fast tests, half the soil compressive strength $UCS/2$ should equal Cu in saturated conditions (Hunt, 2007). This allows to potentially locate the water table. T5 (10.6 m) and T6 (18.5 m) were cored in 2007. They were mainly used for laboratory testing on samples and seismic downhole tests, the results of which were already reported (Renalier et al., 2010a). T6 was drilled to a depth of 18 m in 2007. It was operated with the objective of conducting logging operations (Bièvre et al., 2012). Gamma-ray logging (expressed in hits per second, h/s) was conducted in boreholes T4 to T7. Finally, T8 was cored in September 2011 down to a depth of 25.8 m and gamma-ray logging was performed. Classical identification tests were conducted (water content, grain size, mechanical tests with pocket devices, etc.). The grain size distribution of the fine-grained matrix (<2 mm) was determined by laser diffraction with a Malvern Mastersizer 2000. Organic matter was removed using H_2O_2 (30%). Water was used as a dispersant and samples were stirred and sonicated during a few minutes prior to measurements. Samples were analysed in duplicates to evaluate repeatability. Magnetic Susceptibility (MS) curves were established using a Bartington MS2 contact

Table 1
Boreholes and parameters used in this study.

Borehole	Coordinates (m, Lambert93)		Date	Elevation (m)/ Depth (m)	Type	Tests	Reference
	Latitude	Longitude					
T0	910,648	6,430,549	Nov 1986	714.9/89	Drilling	DPR (Ar, Df, Tp), Inclinometer (Sep. 1988 to Apr. 1994)	T0 in Jongmans et al. (2009)
T1	910,883	6,430,587	Nov 1986	675.6/59	Coring	Geotechnical tests (grain size), MS, 14C dating, Inclinometer (Sep. 1988 to Jul. 1994)	T1 in Jongmans et al. (2009)
T2	911,033	6,430,576	Nov 1986	650.8/17.25	Coring	Inclinometer (Sept. 1988 to Feb. 1994)	T2 in Jongmans et al. (2009)
T3	910,950	6,430,679	Nov 1986	662.4/20.5	Drilling	DPR (Ar, Df, Tp), Inclinometer (Apr. 1987 to Jul. 1994)	
T4	910,823	6,430,417	Oct 2007	692.6/63	Coring (0–49.3), Drilling (49.3–63)	γ-ray logging, geotechnical tests (water content, Unit weight, USS, UCS), MS, 14C dating	D1 in Bièvre et al. (2012)
T5	910,543	6,430,357	Oct 2007	742/10.6	Coring	γ-ray logging	T5 in Bièvre (2010)
T6	910,816	6,430,416	Oct 2007	694.7/18.5	Coring	γ-ray logging	T8 in Bièvre (2010)
T7	910,832	6,430,420	Oct 2007	689.2/18	Drilling	γ-ray logging	D3 in Bièvre et al. (2012)
T8	910,894	6,430,371	Sep 2011	674.4/25.8	Coring	Geotechnical tests (water content, unit weight, Grain size, USS), MS, AMS, γ-ray logging Inclinometer (Jul. 2014 to Oct. 2015)	
T9	911,012	6,430,711	Nov 1986	640/15.5	Drilling	DPR (Ar, Df, Tp)	

DPR: drilling parameter recording; Ar: advance rate; Df: drilling fluid pressure; Tp: thrust pressure; MS: Magnetic Susceptibility; AMS: Anisotropy of Magnetic Susceptibility; USS: unconfined shear strength; UCS: unconfined compressive strength.

sensor on cores T1, T4 and T8, at a 1 cm (T8) and 2 cm (T1, T4) spatial resolution when the quality of recovery was enough. Discrete sampling within 8 cm^3 non-magnetic plastic boxes were performed on core T8. The Anisotropy of Magnetic Susceptibility (AMS) was measured on a total of 70 samples using an AGICO MFK1-FA Kappabridge (spinning specimen method). For each sample, these measurements allowed to reconstruct the AMS tensor defined by three eigenvectors (*Kmax*, *Kint* and *Kmin*) and the mean magnetic susceptibility (*Km*) (Tarling and Hrouda, 1993). Following Jelinek (1981), the AMS fabric is usually illustrated using parameters such as the foliation ($F = Kint/Kmin$), the lineation ($L = Kmax/Kint$), or the shape parameter. This fabric is usually comparable to the sediment fabric (Rochette et al., 1992) or to the orientation of tectonic structures (Borradaile and Henry, 1997).

4. Results

4.1. Chronology

Chronological results are presented in Fig. 4a. Lacustrine and till sediments were deposited on a palaeoterrace originating from the Riss glaciation older than 100 ka. A global trend is observed from the base to the top of the sequence with ages ranging, respectively, between 40 and 50 ka and between 30 and 40 ka. They suggest a functioning of the lake during around 10 ka and with a sedimentation rate of ~1–1.5 cm/yr. These ages agree with previous findings (e.g., Monjuvent, 1973, see Table S1 in Supplementary Information S-1]monjuvent1973a. OSL dates range between 20 and 50 ka and appear of little confidence, at least for the youngest age (20–30 ka). However, several outliers are visible on the figure. First, core T1 suggests ages younger by ~5–10 ka for these lacustrine deposits (location of the borehole in Fig. 2c). A shift of these samples toward the top by around 70 m (Fig. 4b) sets them in agreement with the rest of the dates. This suggests that clay and till layers in the vicinity of T1 could have slid and are now located ~70 m lower than their original position. This hypothesis will be discussed further in the paper. Finally, 2 other outliers with young ages compared to the sediments are observed. They correspond to plant remains found at outcrop in the neighbouring Harmalière landslide (Ly-2527) and at 28.5 m depth in coring T4, both within lacustrine deposits. The young ages (500–515 yr cal BP for Ly-2527 and 265–310 or 145–215 yr cal BP for T4) suggest that they date reactivation phases.

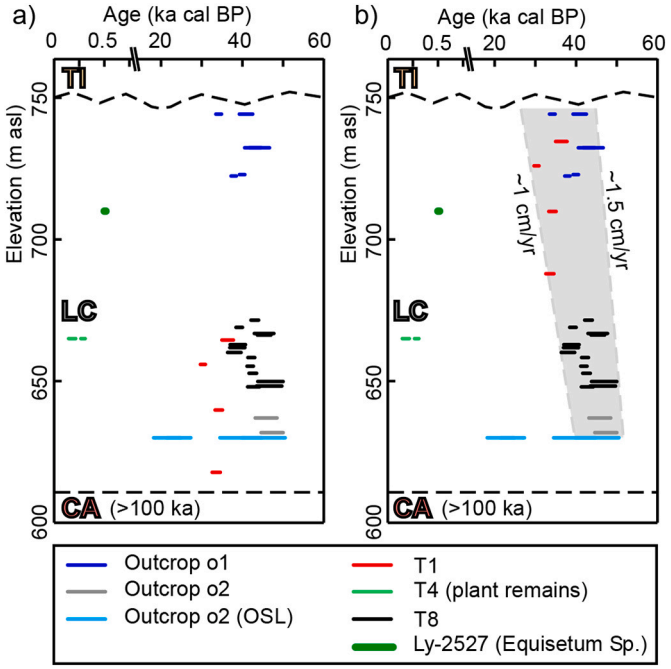

Fig. 4. ^{14}C and OSL dating on the study site. CA: compact and cemented alluvium (age from Monjuvent, 1973); LC: laminated clays; TI: till. a) Original data. b) The same with a 70 m upward shift of samples from core T1.

4.2. Boreholes

Among the ten boreholes used in this study, only T0, T1, T4 and T8 are presented below in detail. The others (T2, T3, T5, T6, T7 and T9) that are shorter and usually performed without coring, present monotonic facies and are not detailed in the paper. They were, however, used for the geological interpretation. The data are summarized below and detailed in Supplementary Information S-2. Coring T2 had a very poor recovery (close to 0 in average) except between 4.5 and 6.75 m (25%) and 14.5 to 17.25 m (almost 100%). As such, only these two levels can be analysed, the deepest one corresponding to till and the other probably

to clays (a detailed log is provided as Supplementary Information in Fig. S3). In the same way, T3 and T9 mainly correspond to till and are presented in Figs. S5 to S7. Finally, T5, T6 and T7 in which only gamma-ray logging has been performed were used to establish lateral correlations and they are detailed in Supplementary Fig. S8.

4.2.1. T4

The log of T4 is presented in Fig. 5 and some photographs are presented in Fig. 6. It shows alternation of layers of till (0–3.5 m and 11.7–19 m) and lacustrine deposits (3.5–11.7 and 19–63 m). Lacustrine deposits correspond to the typical laminated clays (Fig. 6a) and exhibit gamma-ray >85 h/s and almost constant MS values around 20 (Fig. 5a). The till is made of a fine-grained matrix with also sand and gravels. Pebbles of carbonated and endogeneous rocks (e.g. gneiss) frequently striated are also observed (Fig. 6b). Gamma-ray is lower in the till (<80 h/s) than in LC and MS is higher (>30) along with heterogeneous pattern, indicating a higher content in detritic material (gravels). Dipping, distorted and faulted laminae along with slumped layers and sand beds are observed all along the lacustrine levels. However, they are much more concentrated at the top of each lacustrine unit. Dropstones

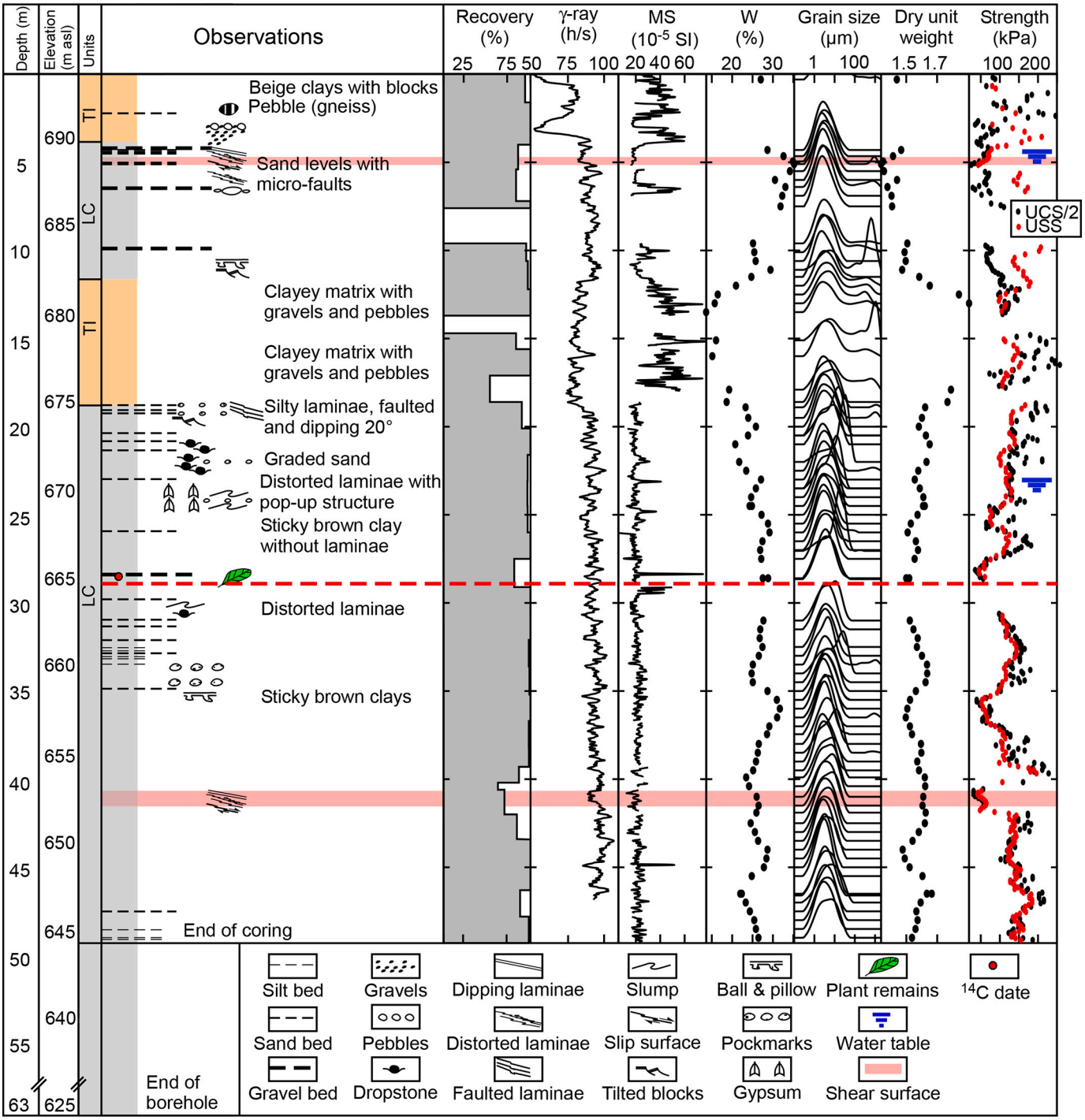

Fig. 5. Log of T4 (location in Fig. 2c). Water table levels from OMIV Observatory (RESIF/OMIV, 2006). Red dashed line: inactive shear surface dated 145–310 yr cal BP (see text for details). Pink stripes: active shear surfaces. *UCS*: unconfined compressive strength; *USS*: unconfined shear strength. (For interpretation of the references to colour in this figure legend, the reader is referred to the web version of this article.)

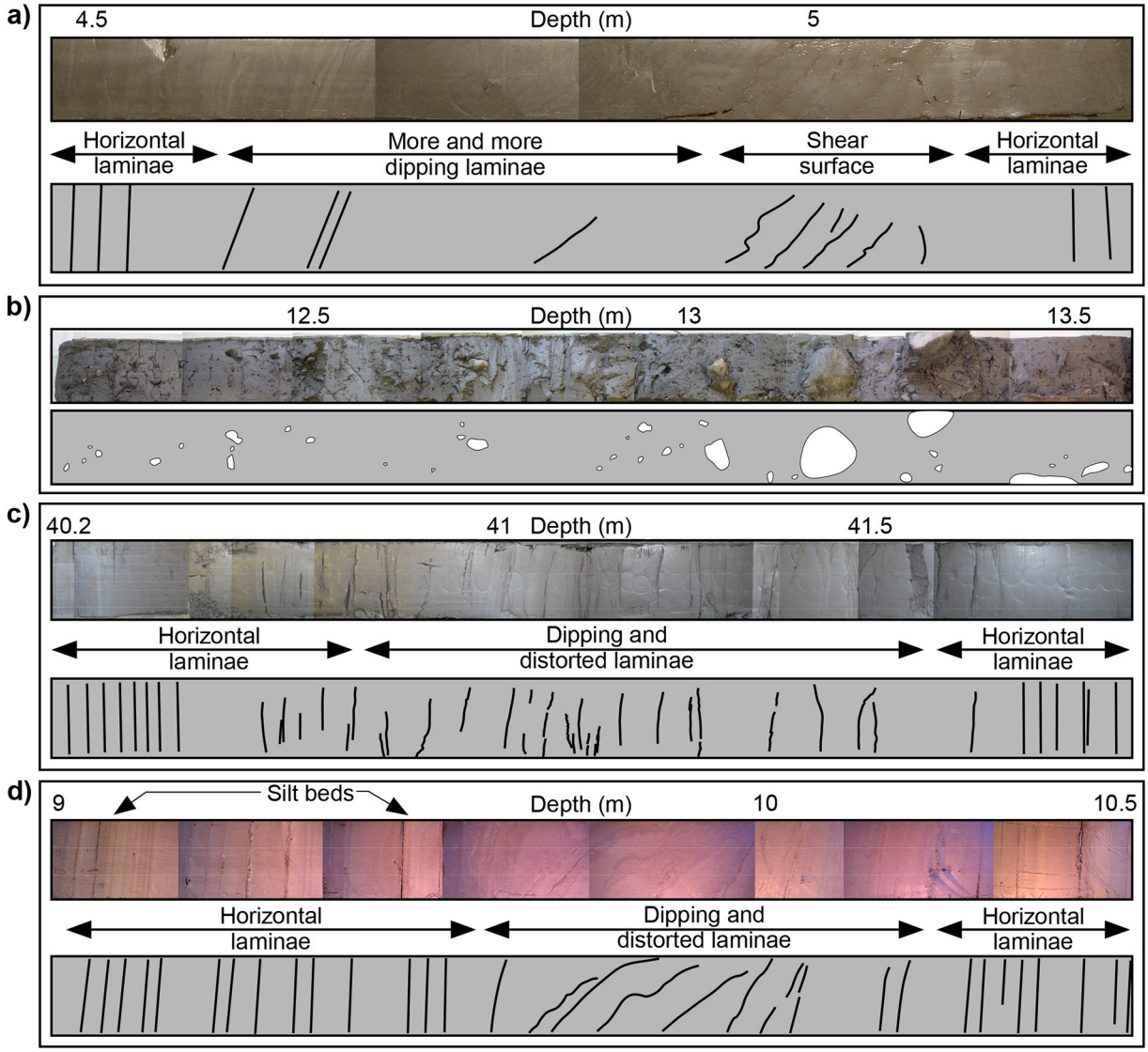

Fig. 6. Photographs of lithological facies in T4 and T8. a) Laminated clays with a shear surface at 5 m depth in T4. b) Till in T4. c) Laminated clays with a shear surface between 40.5 and 41.5 m depth in T4. d) Laminated clays with a shear surface between 9.6 and 10.2 m in T8.

are also observed with an increase in concentration at the top of each lacustrine unit, i.e. just below the till. These observations suggest that the closer the glacier, the higher the number of dropstones and the higher the occurrence of synsedimentary deformation generated by the southward motion of the glacier (and vice-versa). Grain size curves of the fine-grained matrix indicate a globally unimodal distribution corresponding to silty clays (Fig. 5). Water content is high from surface down to 7.5 m (>30%). It then shows a decrease until between 12 and 18.5 m where it is lower than 20%, and then a further increase up to 28% at 28.6 m depth. This pattern is anti-correlated with dry unit weight, suggesting a lower water content in till, in agreement with gamma-ray and MS curves. Below 28.6 m and down to 49 m, the curve presents variations but a global decreasing trend from 28 to 24% (−0.15% per m). The undrained shear strength *USS* is equal to half the compressive strength (*UCS*/2) between 4.5 and 5 m and below 23 m. This equality indicates saturated conditions and allows to locate two water tables. This is in very good agreement with piezometric data (RESIF/OMIV, 2006).

Two shear surfaces were visually identified in T4 at depths of 4.75–5.10 m and 40.7–41.5 m (Fig. 6a and c, respectively). The laminae show a progressive increase in dipping when approaching distorted laminae indicative of the location of the shear surface. The undrained shear strength varies between 20 and 250 kPa all along the core. Close examination of the data allows to determine several trends in *USS* versus depth distribution. In the LC unit below 18.5 m and down to 28.5 m, *USS* decreases more or less regularly from 160 to 40 kPa. Further, and down to 49.3 m it increases progressively up to ca 150 kPa. Apart from this apparent trend, very low values (<50 kPa) are present in the vicinity of the deep shear surface. It should also be noticed that high values (>200 kPa) occur immediately above the shear surface. The same behaviour is also visible around the upper shear surface (~5 m depth). Low *USS* values associated with shear surface have been also observed in Italian mudslides (Picarelli et al., 2005). The apparent increase in shear strength below 28.5 m suggests that these clayey layers have been very fewly remolded by the landslide activity.

On the contrary, the trend in *USS* above 28.5 m suggests than the clays have been remolded. A plant remain was found at 28.5 m depth (Figs. 4 and 5) and provided a 2σ ^{14}C age of 145–214 or 267–309 yr cal BP. This result supports *USS* findings and furthermore specify that the first 28.5 m in this area most probably slid during one of these 2 periods, during the Little Ice Age. Finally, this global interpretation is in good agreement with the decrease of water content from 28.5 m down to 49.3 m that can be simply explained by an increase in sedimentary compaction and a subsequent decrease of porosity.

4.2.2. T1

T1 was cored in 1986 and stored without caution in wood cases during several decades before being studied in the mid-2010s. It explains the limited amount of measurements that could be conducted (Fig. 7). Similarly to T4, it shows alternations of till and lacustrine units, illustrated by variations of MS. The systematic petrographic analysis of clasts >2 mm shows a similar proportion of carbonates versus endogenous rocks (60% vs. 40%) in the different till units. It suggests a deposition by the same glacier. The abundance of dropstones in the laminated clay unit also suggest the proximity of the glacier. Laminae dipping between 20 and 40° are observed between 18 and 40 m depth. The layers around the strongly dipping laminae (between 32 and 40 m depth) are associated to normal faults, abrupt changes in the dip angle with no gradual evolution and fluid escape features. Finally, this 8 m-thick disrupted sequence is capped by slumps, indicative of synsedimentary deformation (Fig. 7). It is, however, difficult to assess the origin of this synsedimentary deformation: aquatic landslide caused by sedimentary overload or by the southward movement of the glacier?

The inclinometer tube could not be sealed at the bottom of the borehole, probably because of collapse of sediments in the upper part of the till unit below 45 m depth. However, three main active shear surfaces were determined from inclinometer data, at depths of around 15, 35 and 40–43 m (Fig. 7) and almost 50% of the cumulative displacements are accommodated by the deepest shear surface.

4.2.3. T8

Fig. 8 presents the log of T8. The lithology is monotonic and mainly shows lacustrine clays without gravels or pebbles (except at a depth of ~2 m). 3 disrupted levels were observed on core samples at depths ranges of 1.7–2.3 m, 4.2–4.5 m and 9.6–10.2 m (Fig. 8). A photograph of the shear surface at 9.6–10.2 m is presented in Fig. 6d. These observations are in good agreement with inclinometer data for the first and third surfaces. The second surface (4.2–4.5 m) does not show displacement on the inclinometer curve between late July 2014 and early October 2015 and may then be currently inactive. Finally, a fourth shear surface is evidenced from inclinometer data only (i.e. not observed on core samples) at around 14 m depth but was not observed on samples. A small lack of recovery may correspond to it. Inclinometer data indicate that 65% of the observed deformation is accommodated by the uppermost shear surface (1.7–2.3 m), 0% by the second one (4.2–4.5 m), 25% by the third one (9.6–10.2 m) and, finally, the last 10% by the deepest shear surface (~14 m). However, it must be stressed out that the inclinometer did not reach the base of the landslide, located at a depth of around 45 m in T4 (Fig. 5). The log shows dry unit weight gently increasing from ~1.6 g.cm^{-3} at surface to ~1.65 g.cm^{-3} at 25.8 m depth. The average *USS* is around 100 kPa with a standard deviation of 30 kPa. 3 zones present outlying values corresponding to the identified shear surfaces. Low *USS* is observed between 1.5 and 2.4 m (65 kPa) and between 4.2 and 4.5 m (25 to 50 kPa). On the contrary, higher *USS* is found for the shear surface between 9.6 and 10.2 m (162 ± 12 kPa in average). Below

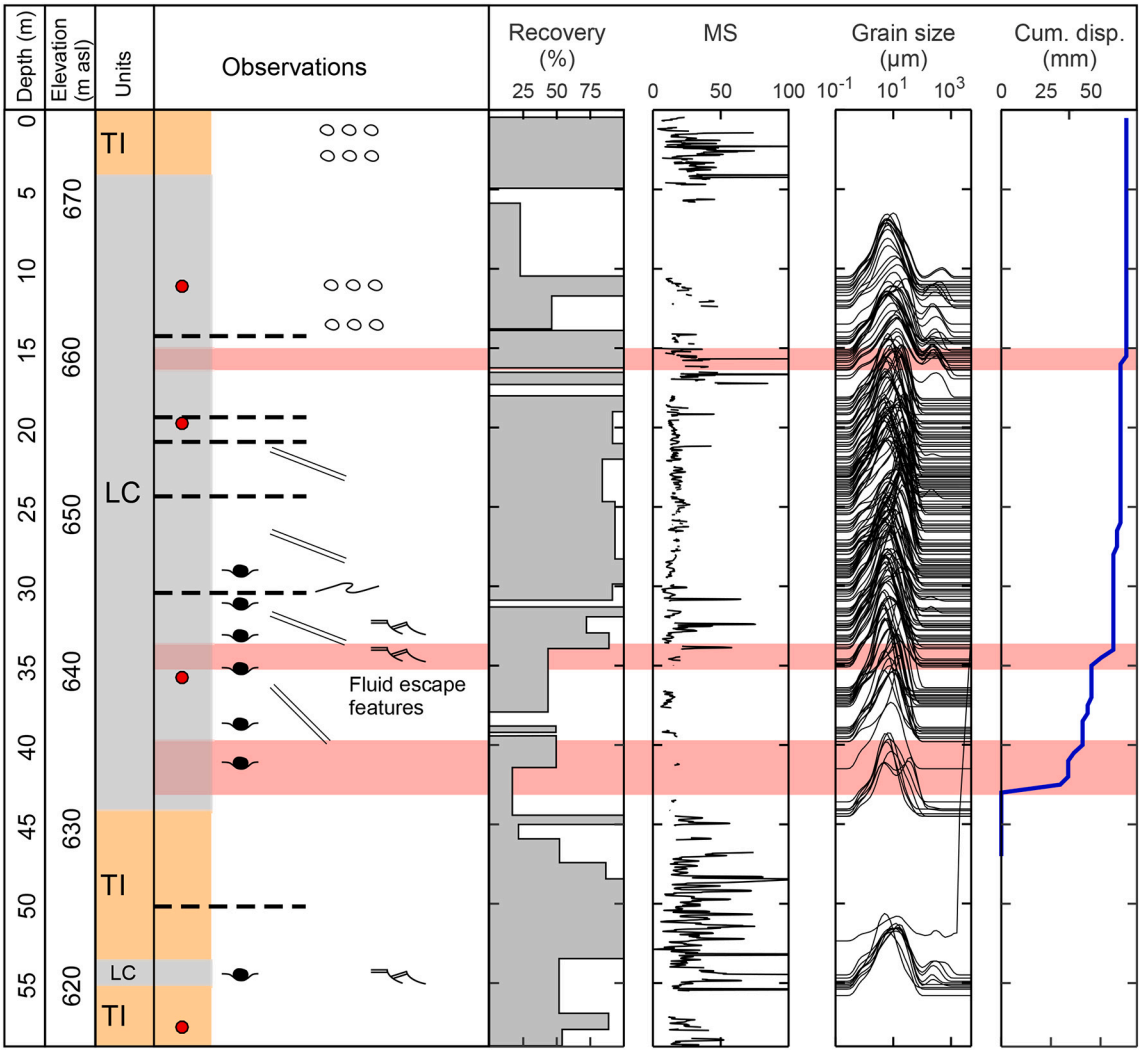

Fig. 7. Log of coring T1 (location in Fig. 2c). Same legend as for Fig. 5.

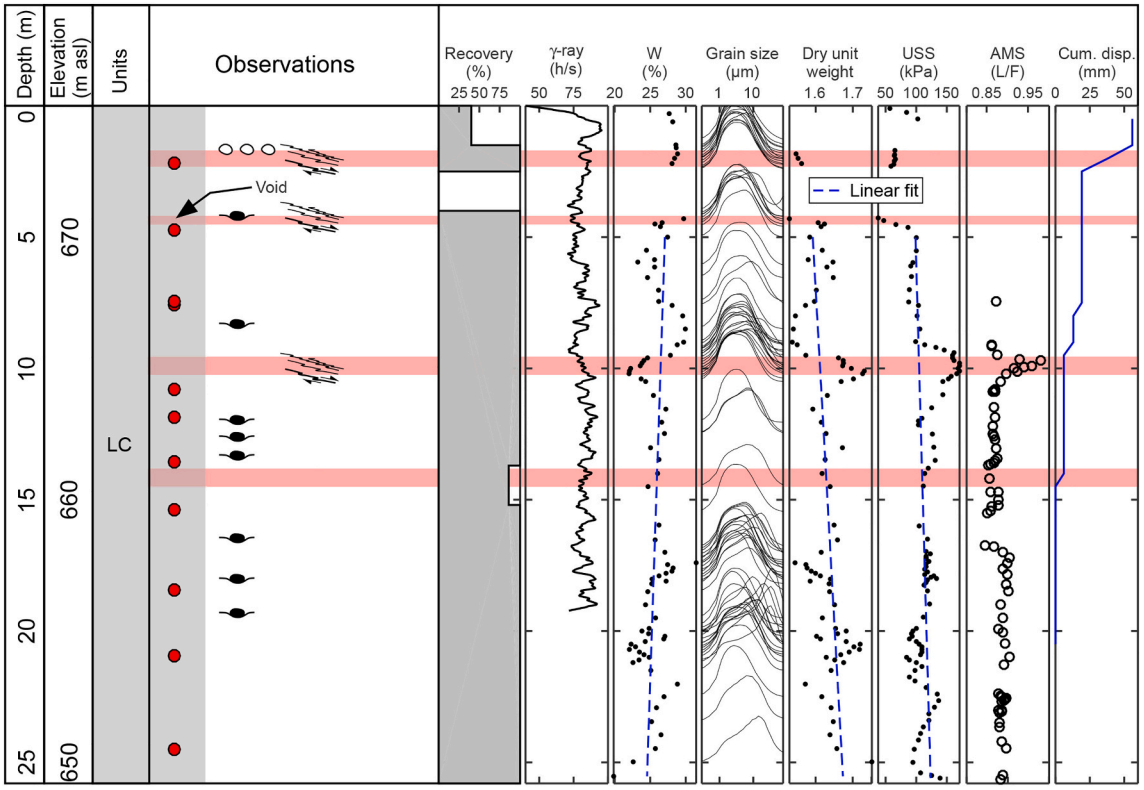

Fig. 8. Log of coring T8 (location in Fig. 2c). Red stripes: shear surfaces observed on cores. Blue dashed lines: linear fits. Inclinometer cumulated displacements between 23 July 2014 and 07 October 2015 (1.2 yr). (For interpretation of the references to colour in this figure legend, the reader is referred to the web version of this article.)

5 m depth and down to the bottom of the borehole, a progressive increase of *USS* (1.2 kPa/m) is observed, along with a progressive decrease of *w* (and, hence, of porosity) of around 0.12%/m, similar to observations in T4. The shear surface at depth is also evidenced by AMS. Values are around 0.85 (from the top to 15 m depth) and 0.9 (from 15 m to 25.6 m depth). *L/F* values progressively increase to more than 1 from 9.5 to 10 m and then progressively decrease. This change from an oblate to a prolate shape of the AMS ellipsoid suggests a stretching and/or a particular orientation of phyllosilicates in the shearing zone.

4.2.4. T0

The main objective of this 89 m-long drilling (no core) was to set an inclinometer below the deepest shear surface. DPR were here used to identify the lithological units. Original DPR data are shown as grey

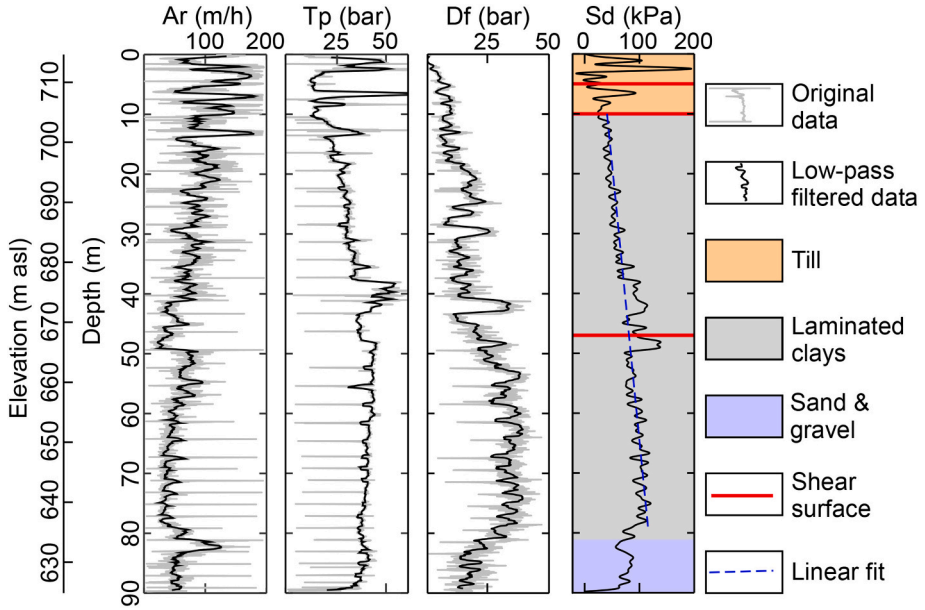

Fig. 9. Drilling Parameter Recording along with the geological and geotechnical interpretation of drilling T0 (location in Fig. 2c). *Ar*: advance rate; *Tp*: thrust pressure; *Df*: drilling fluid pressure; *Sd*: Somerton index. Shear surfaces are from inclinometer data in Jongmans et al. (2009).

curves in Fig. 9. Data were first low-pass filtered, notably to reduce the effect of the adjunction of drilling rods each ~3 m and the results are shown as black curves. The Somerton index *Sd*, computed using Eq. (1), shows 3 main units. From the surface down to around 10 m depth, *Sd* is highly heterogeneous and ranges between almost 0 and 200 kPa, indicative of alternation of fine-grained sediments and blocks. This unit is associated to low *Df* values, suggesting a relatively loose state. Between 10 and 80 m depth, *Sd* shows a progressive and linear increase of 1.1 kPa/m (blue dashed line in Fig. 9) from 35 to 115 kPa. It is noticeable that this trend is not visible on the original DPR curves but is clearly observable when combining them into a mechanical proxy, namely *Sd*. This increase is in agreement with findings of Bartetzko and Kopf (2007) and with observations along T4 and T8. However, two specific zones present *Sd* values higher than the trend, between 37.5 and 43.5 m and between 47 and 49.5 m deep, respectively. These two zones are associated with highest *Df* values. Below 80 m and down to the end of the drilling, *Sd* and *Df* are almost constant at around 80 kPa and 20 bars, respectively, suggesting a homogeneous lithology along with a higher permeability than the overlying units. The top of this unit is located at an elevation of 635 m asl that matches the top of alluvial layers observed at outcrop o2 (Fig. 3). Therefore, those low values of *Sd* and *Df* are interpreted as originating from the presence of sand and gravel slightly subject to compaction and more permeable than the overlying clayey unit.

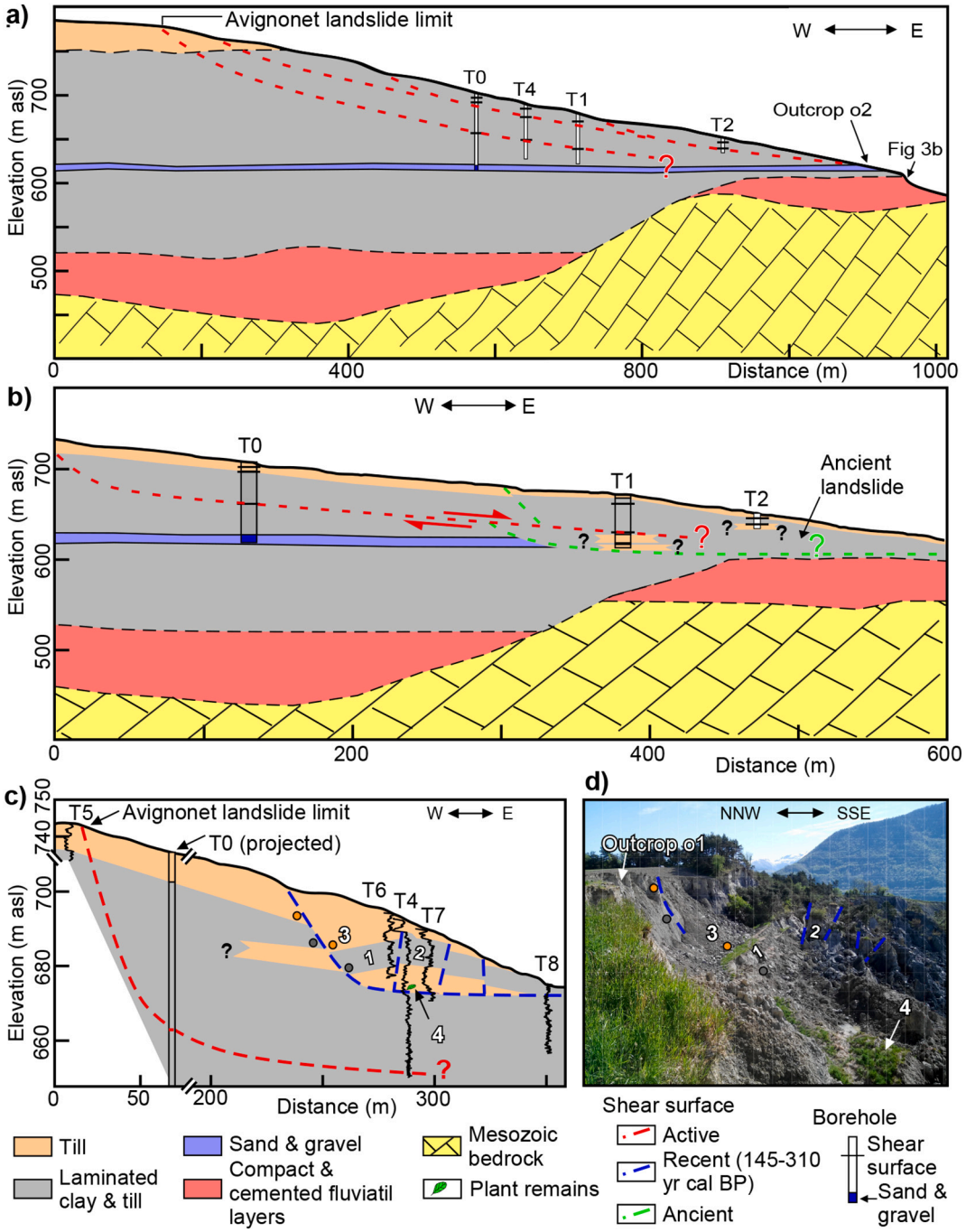

Fig. 10. Geological cross-sections (location in Fig. 2a and c). a) Cross-section 1. b) Cross-section 2. c) Cross-section 3. d) Present-day analogue on the Harmalière landslide (picture shot 10 May 2017). 1: back-tilted block; 2: forward tilted block; 3: filling with till; 4: vegetation.

5. Interpretation

Interpretative geological cross-sections were built using outcrops, corings and lithological reconstruction from DPRs. They are labelled from 1 to 3 (location in Fig. 2a and c) and are presented in Fig. 10. Cross-section 1 (Fig. 10a) stands for an ideal W-E cross-section, without any marked landslide activity. At the base, it shows the Jurassic bedrock, incised by the Drac river and overlain by coarse fluvial material deposited prior to the last glaciation. For a complete description and chronology of those alluvium, we refer to Monjuvent (1973). Once the ice-dammed lake was set, deposits of lacustrine clays alternating with till are found in place. These layers would have been deposited during the maximum of the Würm II glacial stage that should correspond to the global MIS2. Uncemented layers made of lacustrine sand (with dropstones, mud clasts and mud lenses indicative of synsedimentary deformation) and gravel are visible along outcrop o2 at 625–635 m asl (Fig. 3). They can also correspond to coarse lacustrine filling such as deltaic sand as observed at the Charlaix site (CH in Fig. 1; Bièvre et al., 2018) and on an outcrop a few hundred m north of the Charlaix site ("ravin des Garguettes"; Monjuvent, 1973). Finally, after the glacier retreat and the erosion of both the till and the lacustrine clays by the Drac river, shear surfaces developed in the sedimentary sequence. The two deepest ones (15 m and 45 m) are drawn in Fig. 10a.

Two further cross-sections (labelled 2 and 3 in Fig. 1b) are located 150 m north and south from cross-section 1, respectively. They both evidence a loss of lateral continuity in the eastern part of the sedimentary sequence, contrary to cross-section 1. At 300 m along cross-section 2 (Fig. 10b) a disruption is observed in the previously proposed sedimentary sequence. Alluvial layers were not observed at depth in coring T1. Also, till levels in the bottom part of T2 (where recovery was enough to interpret the lithology) were not observed at a similar elevation in T1. Finally, based on ^{14}C dates in T1, an upward translation of ~70 m of this coring would allow to find dates in agreement with the other data from the sedimentary sequence (Fig. 4). This hypothesis suggests that this zone could have undergo a more or less localized landslide event with a downward displacement of ~70 m. The timing of this specific slide event is, however, unknown so far. Cross-section 3 is located about a hundred meters south of cross-section 1 (location in Fig. 1b). Once again, it is difficult to establish lateral correlations assuming an initial more or less horizontal stratification. Coring T4 shows alternation of laminated clays and till mixed with lacustrine clays, whereas T8 exhibits lacustrine clays (Fig. 10c). Gamma-ray logging in T4, T5, T6 and T8 confirms this lack of lateral continuity. However, the observation of the main scarp of the neighbouring Harmalière landslide (reactivated in late June 2016; location in Fig. 2a) in May 2017 (Fig. 10d) allows a plausible interpretation of cross-section 3. The recent reactivation shows the presence of rigid blocks tilted backward and forward (numbers 1 and 2), separated by discontinuities, with a filling by a mix of till with a few amount of laminated clays (number 3). The downward movement (15 to 30 m in the case of the Harmalière landslide in June 2016, Fig. 10d; Lacroix et al., 2018) implied the same movement of the upper soil and of the vegetation (number 4). It is then hypothesized that the southern part of the Avignonet landslide underwent a similar deformation.

The three previously established interpretative cross-sections suggest a multi-phase activity of the southern part of the Avignonet landslide. A conceptual model of its evolution is presented in Fig. 11 (left column) along with corresponding N-S geological cross-sections in the right column of the figure. Fig. 11a presents the Avignonet area during the Last Glacial Maximum, around 30–40 ka cal BP after chronological results, which was at the front of the Romanche glacier. Northward (retreat) and southward (advance) movements of the glacier (and of the shoreline of the palaeolake) were induced by climatic oscillations and are illustrated by the lateral indentation between the lacustrine laminated clays and the till mixed with laminated clays. After the glacier definitive retreat, the date of which remains unknown but which occurred after 30–40 ka cal BP and which left a subsequent thickness of till, the Drac river started to erode deeply into the soft till and clayey units (Fig. 11b). This deep erosion was probably sufficient to allow the initiation of landsliding. This is illustrated in Fig. 11c where a massive landslide inducing a vertical motion of around 70 m, as suggested by ^{14}C ages in T1, at a time unknown, occurred on the northern side of the Avignonet landslide. This activation phase washed out a part of the fluvial layers observed between 625 and 635 m asl and explains their absence in T1. In term of hydrogeology, the occurrence of a permeable fluvial alluvial layer at the bottom of T0 suggests that this layer drains water which is then trapped in the eastern part of the landslide. This trapped aquifer may have provided water able to help the landslide motion by lubricating the shear surfaces. After a period of erosion and probable landsliding activity, another well-documented landslide was activated in the southern part of the studied cross-section in recent time. This is attested by ^{14}C age (145–215 or 265–310 yr cal BP with a 2σ range) on plant remains at 28.5 m depth in T4 (Fig. 11d). This activation phase, which took place between 1640 CE and 1805 CE at the end of the Little Ice Age is in agreement with another date in the nearby Harmalière landslide (Ly-2527 in Fig. 4; Evin et al., 1985). Stalks of *Equisteum* sp. found in clays suggest a reactivation phase dated 500–515 yr cal BP, i.e. at the beginning of the XIXth century. Finally, an unsourced local newspaper reported by Blanchet (1988) indicated a reactivation of the Avignonet landslide around 1850 CE. All the results gained in this study support the high lithological variability induced by the geological history of the site during the deposition of the sediments and also because of the different landslide phases that occurred after the glacier retreat. This high variability induces a complex behaviour of the landslide. However, several issues remain in the understanding of the Avignonet landslide. Because borehole campaigns were concentrated in the inhabited part in the south of the landslide, no direct observation is available on the rest of its surface. Notably, it is still unknown whether coarse sedimentary layers between 700 and 750 m in elevation (evidenced by geophysics; Bièvre et al., 2016) are made of till or coarse lacustrine deposits.

6. Synthesis and conclusion

Ten boreholes (drillings and corings) acquired between the mid 80s and the mid 2010s were reprocessed and reinterpreted, along with outcrop observations, to establish a geological and geotechnical model of the southern part of the Avignonet landslide in the Trièves area (French western Alps).

The lithology was primary reconstructed using corings. Measurements (e.g. mechanical tests such as undrained cohesion) calibrated on 2 corings allowed to interpret Drilling Parameter Recording from 4 other drillings in terms of lithology and to distinguish between till, laminated clays ans fluvial layers. More precisely, the Somerton index *Sd*, indicative of a mechanical strength, showed trends and orders of magnitude comparable to the undrained shear strength *USS* (which is the cohesion *Cu* in saturated conditions) measured with a pocket vane tester on core samples. The drilling fluid pressure *Df* is in agreement with these interpretations. Finally, Magnetic Susceptibility measurements *MS*, along with gamma-ray logging, allowed to distinguish between the lacustrine clays and the till mixed with lacustrine clays. For this paraglacial geological setting, it could be proposed to conduct drillings with measurement of DPR (at least the advance rate, the thrust pressure and the drilling fluid pressure) and logging (at least magnetic susceptibility and gamma-ray) to be able to identify with confidence the different lithological units. These parameters were also able to detect remolded strata, notably by identifying disruptions of the sedimentary compaction pattern with depth. The methodology used in this work could then be applied to other Quaternary sediments which were submitted to sedimentary compaction, such as lacustrine or coastal environments, to detect deformations of the sedimentary pattern. However, contrary to coring, drilling does not allow to get samples to perform dating. This chronological observation turned out to be crucial to interpret the data

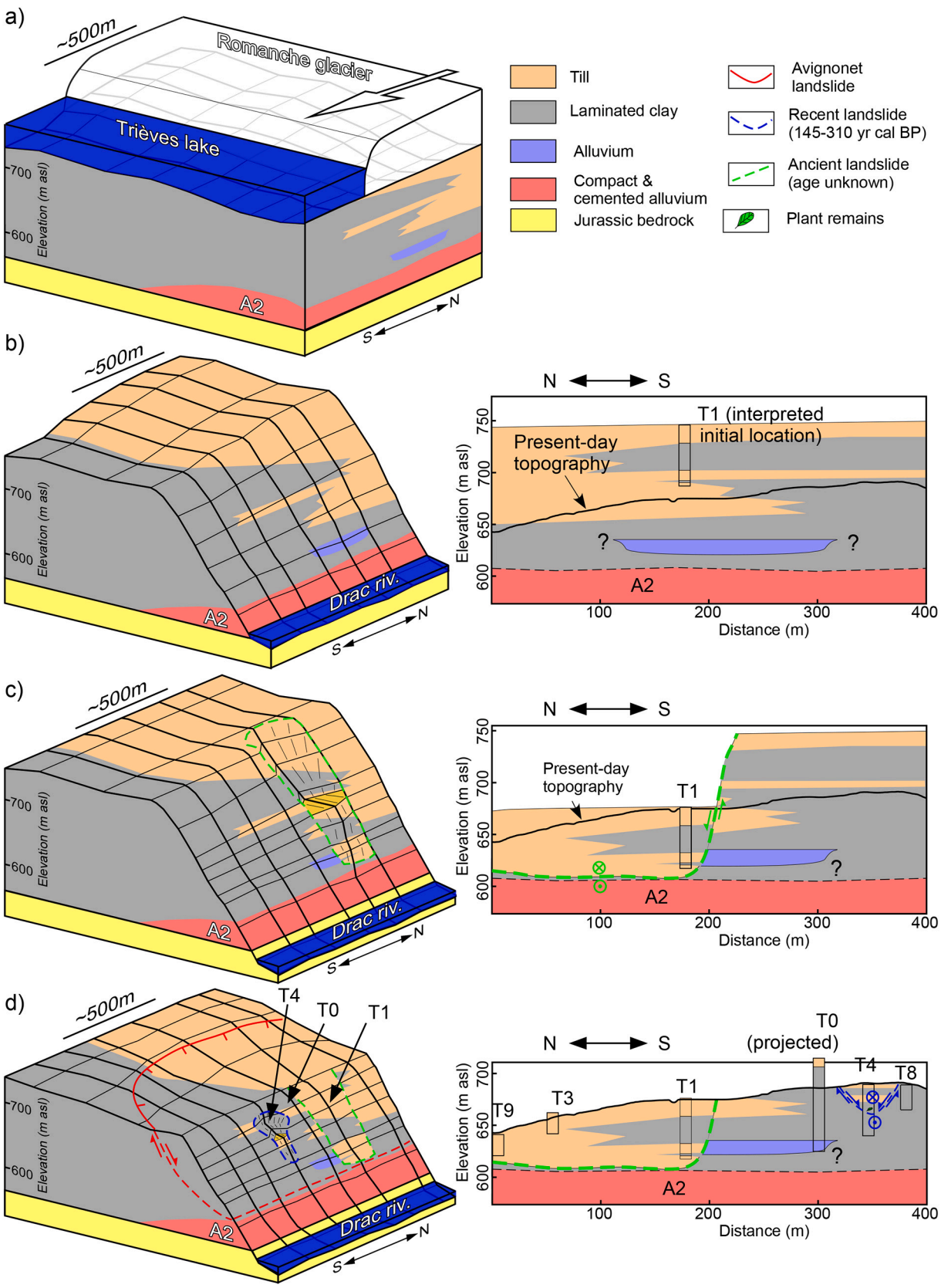

Fig. 11. Scenario of the evolution of the southern part of the Avignonet landslide. Left column: 3D conceptual blocks. Right column: N-S geological cross-sections (location in Fig. 2a and c). a) Situation during the Last Glacial Maximum; b) Situation after the glacier definitive retreat. c) 70 m downward movement of the northern part (timing unknown). d) 28 m downward movement at the end of the Little Ice Age and present-day situation. Boreholes are indicated along with the limits of the Avignonet landslide.

and to build the conceptual model of the evolution of the Avignonet landslide, notably by identifying two previous reactivation phases.

Easy and cheap tests such as *UCS* and *USS* conducted with pocket devices also provide observations on the degree of saturation. On the study site, these measurements showed the presence of two distinct water tables in agreement with piezometer data. In landslide studies, this information is of primary importance. Then, these simple measurements provide a quick and efficient way to determine the presence of one or several water tables. They can further be used to optimize the number and depth of piezometers to be set in the field. Finally, more complex tests such as the anisotropy of magnetic susceptibility, showed the ability of the technique to detect shear surfaces through the reorientation of clay minerals at depth following shearing. This technique, however, cannot be considered as easy to deploy and cost-effective for the engineering community.

Results show that the site presents a high lithological complexity. It originates from the activity of the landslide (past and present) but also from the quaternary geological history with the fluctuations of the glacier, inducing strong vertical and lateral variations. Geological results suggest a multi-phase deformation and landslide activities. It started during the deposition of the laminated clays since they were deformed by glaciotectonism during the maximum Würmian extension. Altogether, this study shows the importance and the relevance of a multi-disciplinary and multi-proxy approach to better constrain the geological setting and the geotechnical implications of landslides in Quaternary periglacial sediments.

Credit author statement

Grégory Bièvre: Conceptualization, funding, data acquisition, processing and interpretation, writing, figures drawing.

Christian Crouzet: conceptualization, funding, data acquisition, processing and interpretation, writing.

Declaration of Competing Interest

The authors declare that they have no known competing financial interests or personal relationships that could have appeared to influence the work reported in this paper.

Acknowledgements

Water table data were provided by the French National Multidisciplinary Observatory on Versant Instabilities OMIV (www.ano-omiv.cnrs.fr). Drillings T4 to T8 were operated by CEREMA Autun (France) benefiting from grants from Université Gustave Eiffel (research programs “Drought” and “Landslides”). Inclinometer measurements in T8 were conducted by CEREMA Lyon (France). Most of ^{14}C ages were determined at Laboratoire de Mesures du Carbone 14 (LMC14, CEA-CNRS-IRD-IRSN-MCC), France, benefiting from a grant from CNRS-INSU. Christine Oberlin (Centre de Datation par le Radiocarbone, Lyon, France) provided informations on sample Ly-2527. T8 benefited from a grant from the federative structure VOR (Université Grenoble Alpes, France). This work has been supported by a grant from Labex OSUG@2020 (Investissements d’avenir - ANR10 LABX56). The village of Avignonet provided core samples of borehole T1. Analysis and measurements on T4 were performed at the Laboratoire d’Écologie des Hydrosystèmes Naturels et Anthropisés (LEHNA, ENTPE-Université Claude Bernard, Lyon, France) and Thierry Winiarski is acknowledged for granting access to the laboratory. Sedimentological description and magnetic susceptibility measurements on T4 were performed by Marc Desmet (Université de Tours, France). Archives on boreholes and geotechnical prospecting from the 80s and 90s were provided by ONF-RTM38, Grenoble, France. CEREGE laboratory (Université Aix-Marseille, France) is acknowledged for providing access to the palaeomagnetic laboratory for AMS measurements. Christophe Dano (Université Grenoble Alpes) is acknowledged for providing informations and help with geotechnical tests. Finally, the authors thank the editor and three reviewers who helped to increase the quality of this manuscript.

Appendix A. Supplementary data

Supplementary data to this article can be found online at https://doi.org/10.1016/j.enggeo.2021.106073.

References

Barféty, J.C., Debelmas, J., 1967. 796. Vif. In: Carte géologique de la France à 1/50000. BRGM Éditions, Orléans, France.

Bartetzko, A., Kopf, A.J., 2007. The relationship of undrained shear strength and porosity with depth in shallow (<50 m) marine sediments. Sediment. Geol. 196, 235–249. https://doi.org/10.1016/j.sedgeo.2006.04.005.

Becker, D.E., 2001. Geotechnical and geoenvironmental engineering handbook. In: Chapter Site Characterization. Springer, New York, USA, pp. 69–105. https://doi.org/10.1007/978-1-4615-1729-0.

Bièvre, G., 2010. Caractérisation de versants argileux instables dans des conditions hydrogéologiques hétérogènes. Approche géophysique. PhD Thesis. Université de Grenoble, France.

Bièvre, G., Knieß, U., Jongmans, D., Pathier, E., Schwartz, S., van Westen, C.J., Villemin, T., Zumbo, V., 2011. Paleotopographic control of landslides in lacustrine deposits (Trièves plateau, French western Alps). Geomorphology 125, 214–224. https://doi.org/10.1016/j.geomorph.2010.09.018.

Bièvre, G., Jongmans, D., Winiarski, T., Zumbo, V., 2012. Application of geophysical measurements for assessing the role of fissures in water infiltration within a clay landslide (Trièves area, French Alps). Hydrol. Process. 26, 2128–2142. https://doi.org/10.1002/hyp.7986.

Bièvre, G., Jongmans, D., Goutaland, D., Pathier, E., Zumbo, V., 2016. Geophysical characterization of the lithological control on the kinematic pattern in a large clayey landslide (Avignonet, French Alps). Landslides 13, 423–436. https://doi.org/10.1007/s10346-015-0579-0.

Bièvre, G., Joseph, A., & Bertrand, C. (2018). Preferential water infiltration paths in a clayey earthslide evidenced by cross-correlation of hydrometeorological time series (Charlaix, French Western Alps). Geofluids, 2018, 20. doi: https://doi.org/10.1155/2018/9593267. Special issue “The Role and Impact of Geofluids in Geohazards”.

Blanchet, F., 1988. Étude Géomécanique de Glissements de Terrain Dans Les Argiles Glaciolacustres de la Vallée du Drac. Phd thesis. Université Joseph Fourier, Grenoble, France.

Borradaile, G.J., Henry, B., 1997. Tectonic applications of magnetic susceptibility and its anisotropy. Earth-Sci. Rev. 42, 49–93. https://doi.org/10.1016/S0012-8252(96)00044-X.

Cai, G., Liu, S., Tong, L., 2010. Field evaluation of deformation characteristics of a lacustrine clay deposit using seismic piezocone tests. Eng. Geol. 116, 251–260. https://doi.org/10.1016/j.enggeo.2010.09.006.

Caris, J.P.T., Van Asch, T.W.J., 1991. Geophysical, geotechnical and hydrogeological investigations of a small landslide in the French Alps. Eng. Geol. 31, 249–276.

Carrière, S., Jongmans, D., Chambon, G., Bièvre, G., Lanson, B., Bertello, L., Berti, M., Jaboyedoff, M., Malet, J.-P., Chambers, J., 2018. Rheological properties of clayey soils originating from flow-like landslides. Landslides 15, 1615–1630. https://doi.org/10.1007/s10346-018-0972-6.

Clayton, C.R.I., Matthews, M.C., Simons, N.E., 1995. Site Investigation, 2nd ed. Blackwell Publishing, Oxford, England.

Coutterand, S., 2010. Étude Géomorphologique des flux Glaciaires Dans les Alpes Nord-occidentales au Pléistocène Récent: Du Maximum de la Dernière Glaciation Aux Premières Étapes de la Déglaciation. Ph.D. thesis. Université de Savoie, France.

Curzi, P.V., Tonni, L., Gottardi, G., Mandanici, E., 2017. High resolution sedimentological and geotechnical characterization of the late Quaternary deposits in the Italian central Adriatic coast (Tronto River mouth). Eng. Geol. 220, 219–233. https://doi.org/10.1016/j.enggeo.2017.02.007.

Evin, J., Marechal, J., Marien, G., 1985. Lyon Natural Radiocarbon Measurements X. Radiocarbon 27, 386–454. https://doi.org/10.1017/S003382220000713X.

Fiolleau, S., Jongmans, D., Bièvre, G., Chambon, G., Lacroix, P., Helmstetter, A., Wathelet, M., Demierre, M., 2021. Multi-method investigation of mass transfer mechanisms in a retrogressive clayey landslide (Harmalière, French Alps). Landslides. https://doi.org/10.1007/s10346-021-01639-z.

Huff, W.D., 1974. Mineralogy and provenance of Pleistocene lake clay in an alpine region. Geol. Soc. Am. Bull. 85, 1455–1460.

Hungr, O., Leroueil, S., Picarelli, L., 2014. The Varnes classification of landslide types, an update. Landslides 11, 167–194. https://doi.org/10.1007/s10346-013-0436-y.

Hunt, R.H., 2007. Geotechnical Investigation Methods: A Field Guide for Geotechnical Engineers. CRC Press, Boca Raton, USA.

IGN, 2019. Remonter le temps, French Geographic Institute. URL: https://remonterletemps.ign.fr. Accessed 10 September 2020.

Jelinek, V., 1981. Characterization of the magnetic fabric of rocks. Tectonophysics 79, T63–T67. https://doi.org/10.1016/0040-1951(81)90110-4.

Jongmans, D., Bièvre, G., Schwartz, S., Renalier, F., Beaurez, N., 2009. Geophysical investigation of the large Avignonet landslide in glaciolacustrine clays in the Trièves

area (French Alps). Eng. Geol. 109, 45–56. https://doi.org/10.1016/j.enggeo.2008.10.005.
Lacroix, P., Bièvre, G., Pathier, E., Knieß, U., Jongmans, D., 2018. Use of Sentinel-2 images for the detection of precursory motions before landslide ruptures. Remote Sens. Environ. 215, 507–516. https://doi.org/10.1016/j.rse.2018.03.042.
Lade, P.V., 2001. Geotechnical and geoenvironmental engineering handbook. In: Chapter Basic Soil Mechanics. Springer, New York, USA, pp. 7–42. https://doi.org/10.1007/978-1-4615-1729-0.
Laudanski, G., Reiffsteck, P., Tacita, J.L., Desanneaux, G., Benoît, J., 2013. Experimental study of drilling parameters using a test embankment. In: Coutinho, R.Q., Mayne, P. W. (Eds.), Geotechnical and Geophysical Site Characterization 4. Taylor & Francis, London, England, pp. 435–440.
Lee, C.-C., Zeng, L.-S., Hsieh, C.-H., Yu, C.-Y., Hsieh, S.-H., 2012. Determination of mechanisms and hydrogeological environments of gangxianlane landslides using geoelectrical and geological data in Central Taiwan. Environ. Earth Sci. 66, 1641–1651. https://doi.org/10.1007/s12665-012-1522-5.
Lofi, J., Pezard, P., Loggia, D., Garel, E., Gautier, S., Merry, C., Bondabou, K., 2012. Geological discontinuities, main flow path and chemical alteration in a marly hill prone to slope instability: Assessment from petrophysical measurements and borehole image analysis. Hydrol. Process. 26, 2071–2084. https://doi.org/10.1002/hyp.7997.
Lory, C., 1858. Carte géologique du Dauphiné, Isère, Drôme. Hautes Alpes, Imprimerie Lemmercier, Paris, France.
Meisina, C., 2006. Characterisation of weathered clayey soils responsible for shallow landslides. Nat. Hazards Earth Syst. Sci. 6, 825–838. https://doi.org/10.5194/nhess-6-825-2006.
Monjuvent, G., 1973. La transfluence Durance-Isère. Essai de synthèse du Quaternaire du bassin du Drac (Alpes françaises). Géol. Alpine 49, 57–118.
Pécher, A., Barféty, J.C., Montjuvent, G., Carme, F., 1988. 821. La Mure. In: Carte géologique de la France à 1/50000. BRGM Éditions, Orléans, France.
Picarelli, L., Urciuoli, G., Ramondini, M., Comegna, L., 2005. Main features of mudslides in tectonised highly fissured clay shales. Landslides 2, 15–30. https://doi.org/10.1007/s10346-004-0040-2.
Reimer, P.J., Bard, E., Bayliss, A., Beck, J.W., Blackwell, P.G., Ramsey, C.B., Buck, C.E., Cheng, H., Edwards, R.L., Friedrich, M., et al., 2013. IntCal13 and Marine13 Radiocarbon Age Calibration Curves 0-50,000 years cal BP. Radiocarbon 55, 1869–1887. https://doi.org/10.2458/azu_js_rc.55.16947.
Renalier, F., Bièvre, G., Jongmans, D., Campillo, M., Bard, P.-Y., 2010a. Characterization and monitoring of unstable clay slopes using active and passive shear wave velocity measurements. In: Miller, R.D., Bradford, J.D., Holliger, K. (Eds.), Advances in Near-Surface Seismology and Ground-Penetrating Radar Number 15 in Geophysical Developments Series. Society of Exploration Geophysics, Tulsa, USA, pp. 397–414. https://doi.org/10.1190/1.9781560802259.ch24.
Renalier, F., Jongmans, D., Campillo, M., Bard, P.-Y., 2010b. Shear wave velocity imaging of the Avignonet landslide (France) using ambient noise cross-correlation. J. Geophys. Res. 115, F03032 https://doi.org/10.1029/2009JF001538.
RESIF/OMIV, 2006. French multidisciplinary observatory of versant instabilities. In: RESIF - Réseau Sismologique et géodésique Français. 10.15778/RESIF.MT.
Rochette, P., Jackson, M., Aubourg, C., 1992. Rock magnetism and the interpretation of anisotropy of magnetic susceptibility. Rev. Geophys. 30, 209–226. https://doi.org/10.1029/92RG00733.
Rohatgi, A., 2019. WebPlotDigitizer, V.4.2. URL: https://automeris.io/WebPlotDigitizer. Accessed 10 September 2020.
Somerton, W.H., 1959. A laboratory study of rock breakage by rotary drilling. Petrol. Trans. AIME 216, 92–97.
Stuiver, M., Reimer, P.J., 1993. Extended ^{14}C database and revised CALIB radiocarbon calibration program. Radiocarbon 35, 215–230.
Tarling, D.H., Hrouda, F., 1993. The Magnetic Anisotropy of Rocks. Chapman & Hall, London, England.
Uhlemann, S., Smith, A., Chambers, J., Dixon, N., Dijkstra, T., Haslam, E., Meldrum, P., Merritt, A., Gunn, D., Mackay, J., 2016. Assessment of ground-based monitoring techniques applied to landslide investigations. Geomorphology 253, 438–451. https://doi.org/10.1016/j.geomorph.2015.10.027.
Van Asch, T.W.J., Hendriks, M.R., Hessel, R., Rappange, F.E., 1996. Hydrological triggering conditions of landslides in varved clays in the French Alps. Eng. Geol. 42, 239–251.